

Rapid warming in mid-latitude central Asia for the past 100 years

Fahu CHEN (✉)¹, Jinsong WANG^{1,2}, Liya JIN¹, Qiang ZHANG², Jing LI¹, Jianhui CHEN¹

¹ Key Laboratory of Western China's Environmental Systems (Ministry of Education), Lanzhou University, Lanzhou 730000, China

² Institute of Arid Meteorology, CMA, Key (Open) Laboratory of Arid Climatic Changing and Reducing Disaster of Gansu Province (CMA), Lanzhou 730020, China

© Higher Education Press and Springer-Verlag 2009

Abstract Surface air temperature variations during the last 100 years (1901–2003) in mid-latitude central Asia were analyzed using Empirical Orthogonal Functions (EOFs). The results suggest that temperature variations in four major sub-regions, i.e. the eastern monsoonal area, central Asia, the Mongolian Plateau and the Tarim Basin, respectively, are coherent and characterized by a striking warming trend during the last 100 years. The annual mean temperature increasing rates at each sub-region (representative station) are 0.19°C per decade, 0.16°C per decade, 0.23°C per decade and 0.15°C per decade, respectively. The average annual mean temperature increasing rate of the four sub-regions is 0.18°C per decade, with a greater increasing rate in winter (0.21°C per decade). In Asian mid-latitude areas, surface air temperature increased relatively slowly from the 1900s to 1970s, and it has increased rapidly since 1970s. This pattern of temperature variation differs from that in the other areas of China. Notably, there was no obvious warming between the 1920s and 1940s, with temperature fluctuating between warming and cooling trends (e.g. 1920s, 1940s, 1960s, 1980s, 1990s). However, the warming trends are of a greater magnitude and their durations are longer than that of the cooling periods, which leads to an overall warming. The amplitude of temperature variations in the study region is also larger than that in eastern China during different periods.

Keywords arid, central Asia, temperature variation, warming trend

1 Introduction

Global warming has been the focus of significant scientific debate during the last two decades. Numerous studies have established global mean surface air temperature time series for the last 100 years using different methods, of which the CRUTEM2v (Jones, 1994; Jones and Moberg, 2003), the GISS (Hansen et al., 1999, 2001) and the NCDC (Peterson et al., 1998) are three representative time series. The Fourth Intergovernmental Panel on Climate Change (IPCC) Report (Solomon et al., 2007) states that the global average surface temperature has increased, especially since 1950. It is likely that average Northern Hemisphere (NH) temperatures during the second half of the 20th century are warmer than any other 50-year period in the last 500 years and likely the warmest in at least the last 1300 years (Solomon et al., 2007). The rate of warming averaged over the last 50 years ($0.13 \pm 0.03^\circ\text{C}$ per decade) is nearly twice that for the last 100 years, and eleven of the last 12 years (1995–2006) (except 1996) rank among the 12 warmest years on record since 1850 (Solomon et al., 2007).

In China, Wang (1990) established the first regional surface air temperature time series for the period from 1880 to 1990. Later, Lin et al. (1995) and Wang et al. (1998) further established some air temperature series over different regions in China. These studies indicated that air temperature changes in China over the last 100 years were similar to global and/or NH trends. For example, they documented two warming periods—between the 1920s and 1940s and in the late 1970s, in which the former period was particularly pronounced in mainland China (Ding and Dai, 1994; Wang et al., 1998; Qian et al., 2001; Wang et al., 2004). Perhaps even more significant studies from the Tibetan Plateau (Liu et al., 1998; Liu and Chen, 2000;

Wang et al., 2004) showed that the increase in temperature was 1°C higher than that of the global/NH pattern between 1961 and 1990. This warming had also been observed in northern and eastern China, but it was not so pronounced in the Xinjiang Uygur Autonomous Region in northwest (NW) China. The subsequent cooling trend between the 1950s and 1970s was also not evident in NW China. Therefore, temperature changes in these regions over the last 100 years could reflect step-wise warming (Wang et al., 1998; Qian et al., 2001).

Air temperature variations are influenced by a number of factors, such as latitude, altitude and land-sea contrast. Therefore, the regional response of surface air temperatures to recent global warming has come under renewed emphasis in international global change research. Even though a global increased temperature pattern has emerged, there are still considerable discrepancies between regional temperature variations, in particular the differences between the northern and southern hemispheres (Jones et al., 1999; Jones and Moberg, 2003; Folland et al., 2001). In China, Liu et al. (1998) analyzed temperature variations on the Tibetan Plateau and discovered that the general temperature trend increased during the period between the 1920s and 1940s, with significant temperature variation across this area. Annual mean surface air temperature over the Tibetan Plateau increased prior to and was of greater amplitude than that of the NH. Qian et al. (2001) analyzed in detail a temperature time series for the period 1880 to present-day in different regional areas of China (with the exception of Taiwan and the Tibetan Plateau). They discovered that there were similarities among the temperature variations in different regions, but discrepancies still existed. For example, the large arid area in mid-latitude China is predominantly influenced by westerlies and therefore climate change may be different from the humid regions in eastern and southeastern China that are heavily influenced by the Asian monsoon. A tree-ring record from Mongolia indicated that it had been

warming continuously throughout the 20th century in central Asia (Jacoby et al., 1996), with similar temperature variations also observed in instrumental records from NW China (Ding and Wang, 2001). Therefore, there are two questions remaining to be addressed:

- 1) Is the temperature variation consistent within the inland mid-latitude of central Asia over the last 100 years?
- 2) Has the temperature variation been seen in NW China, which is significantly different from that in eastern China but similar to tree-ring records from Mongolia, and has it experienced continuous warming during the 20th century?

Here, by using an Empirical Orthogonal Functions (EOFs) analysis and based on 44-year instrumental temperature records (1961–2003), we reconstructed a 100-year long temperature time series for mid-latitude Central Asia and compared its regional characteristics with other regions.

2 Data and method

2.1 Data

The study area is located between 36°–52°N and 50°–120°E, which includes the arid and semi-arid regions of central Asia, such as Mongolia, NW China and Inner Mongolia of China (Fig. 1). In order to make a regional comparison between those areas influenced by the Asian monsoons, we added the data from sites in the eastern part of northern China. As the boundary of the westerly jet migrates north and south during the summer and winter months, this area is the largest non-zonal arid belt, and is influenced by a complex atmospheric circulation. There are 240 basic (benchmark) meteorological stations within the research area and the monthly mean temperature data are from the database of the Goddard Institute for Space Studies (GISS), NASA. All instrumental meteorological

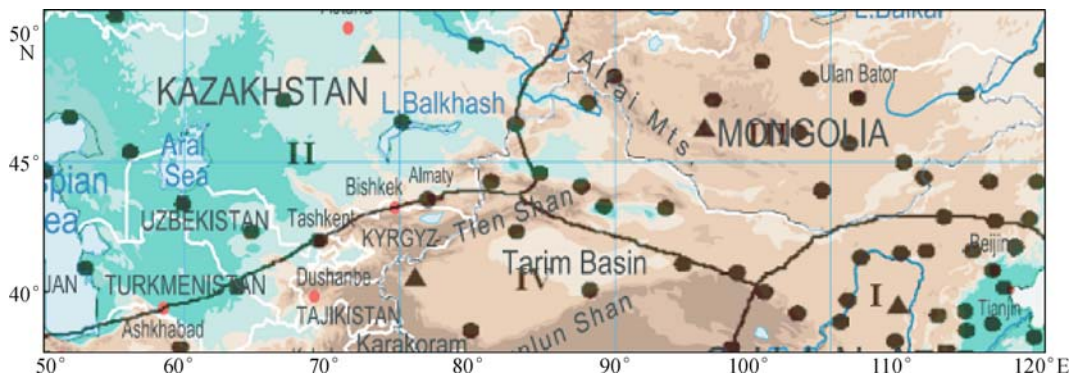


Fig. 1 Distribution of meteorological stations in the research area and the sub-regions according to temperature variations delineated by REOF analysis. Dots = stations; Triangles = central stations; I: East Asia Monsoon Region; II: Central Asia Arid Region; III: Mongolian Arid Region; IV: Tarim Arid Region

data in the database have passed quality control tests (Hansen et al., 1999, 2001). Among the stations, 32 of them are in central Asia, with observational data since 1900. However, most of the data are not continuous and only nine of the 32 stations have complete records of the last 100 years. In China, in particular in the NW, there is a lack of long-term instrumental records, although most stations started continuous observations in the 1960s. Therefore, we preferentially selected the stations that have temperature records continuously from the year 1961 to 2003. Stations with relatively long records or which were located in an area where the meteorological stations are sparse are also included, although there are some obviously questionable data. The data can be interpolated and calibrated by multi-variable linear regression equations. Based on the data quality testing, 69 stations were chosen in this study (Fig. 1) with continuous monthly and annual mean temperature series of 43 years (1961–2003). As shown in Fig. 1, there are many more stations in the eastern part of the study area than in the extremely arid regions, but the overall distribution is relatively even. In order to assess the amplitude of temperature variation, we employed the Climate Anomaly Method (CAM) (Jones, 1994), with the temperature anomaly calculated as the difference of the monthly temperature minus the mean value for the years from 1961 to 1990. Furthermore, we standardized the annual and seasonal mean temperatures, with temperature anomalies divided by the standard deviation, for all the stations from 1961 and 2003.

2.2 Method

2.2.1 Sub-region's division using EOFs

The EOFs and rotated EOFs (REOFs) analyses have been widely used in meteorological studies (Servain and Legler, 1986; Huang, 1988; Kawamura, 1994; Tu et al., 2000). Based on EOFs analysis, fewer numbers of principal components can represent most of the total variance. Furthermore, REOFs analysis can overcome the weaknesses in EOFs analysis by allowing the space field to be expressed by regional characteristics more accurately, while the total variance is left unchanged (Huang, 1988; Kawamura, 1994). In this study, we applied EOFs analysis to the standardized temperature time series to obtain the principal components and their variance contributions. Based on the results of EOFs analysis, REOFs analysis was then performed to obtain the spatial temperature variations of the different sub-regions.

2.2.2 EOF-based temperature series extension

Based on EOFs expansion, an interpolation method (Tu, 1986) was used to extend the temperature time series in most of the stations from 40 years to 100 years. This EOFs-based method has been applied to extended temperature time series successfully in previous studies (Tu, 1986; Zhu et al., 1997; Liu et al., 1998).

In order to evaluate the extended time series, we conducted correlation analyses between the extended time series and the observational time series at nine stations in the study area (Table 1), which have continuous observational data during the past 100 years (test period: 1901–1960). Based on correlation analysis, the extended time series has good relevancy with the observational time series, and there are five stations in which the correlation coefficients are greater than 0.8. These correlations are significant above the 99.9% level for the interval 1901–1960, and the averaged root-mean-square error relative to the observational time series is 0.47, which is in a reasonable range of variation (Table 2).

Table 1 Nine stations which have 100 years of observations (1901–2003)

station code	station name	station position
35121	Orenburg	51.7°N, 55.1°E
35700	Gur'Ev	47.0°N, 51.9°E
36177	Semipalatinsk	50.4°N, 80.3°E
36870	Almaty	43.2°N, 76.9°E
38001	Fort Sevchenko	44.5°N, 50.2°E
38457	Tashkent	41.3°N, 69.3°E
38507	Krasnovodsk	40.0°N, 53.0°E
38687	Cardzou	39.1°N, 63.6°E
54511	Beijing	39.9°N, 116.3°E

3 Results

3.1 EOFs-based reconstruction of extended temperature field

Table 3 shows the first eight principal components representing more than 85% of the total variance, with the first principal component explaining 54.3% of the total variance. The first two principal components account for 64.5% and the first three explain 70% of the total variability. The fourth and subsequent components explain

Table 2 Correlation between extended and observational time series for nine stations

station	35121	35700	36177	36870	38001	38457	38507	38687	54511	average
correlation coefficient	0.81	0.88	0.72	0.69	0.76	0.84	0.87	0.82	0.64	0.78

relatively little change in the total variance. Here we only analyze the first two principal components and their loading vectors, which represent the main features of temperature variation in the study area (mid-latitude central Asia). The EOFs expansion for different seasons (Table 3) also shows that all of the temperature variations in four seasons are similar to the trend in annual mean changes, with the first eight principal components for all four seasons accounting for more than 80% of the total variation explained. The first two eigenvectors (Fig. 2) represent the general reconstructed temperature spatial field. The first loading vector (Fig. 2(a)) is characterized by a positive anomaly, which indicates that the temperature variation in the study area is generally coherent and probably related to the common controlling factor. The second loading vector (Fig. 2(b)) has a different spatial distribution compared with the first one. In Fig. 2(b), the negative anomalies appear in central Asia, including a

small area of NW China (northern Xinjiang Uygur Autonomous Region, China), and the positive anomalies are distributed across the other areas of NW China, e.g. at the bend of the Yellow River in northern China and in Mongolia. This feature represents the difference in climate distribution between the eastern and western areas in this study. For example, when there is an increased temperature trend in most areas of NW China, there will be a decreasing trend in central Asia and a slightly decreasing trend in NE Asia. The first eigenvector for four seasons (not shown) all reflect the same coherency for temperature variations, while the second eigenvector is different in the four seasons, highlighting the differences in temperature changes in the meridional or zonal direction. Meanwhile, the second eigenvector includes both positive and negative anomalies, probably reflecting the different influences of atmospheric circulation patterns in middle to high latitude Asia.

Table 3 The percentage variances of the first 8 principal components (PC) (T = temperature; Accum. var.= accumulated variance)

T types	PC	1	2	3	4	5	6	7	8
annual mean	variance/%	54.3	10.2	6.1	4.1	3.7	2.8	2.0	1.7
	accum. var./%	54.3	64.5	70.6	74.7	78.4	81.2	83.2	84.9
spring	variance /%	43.9	15.1	9.8	6.9	3.4	3.1	2.5	1.6
	accum. var. /%	43.9	59.0	68.8	75.7	79.1	82.2	84.7	86.3
summer	variance /%	36.4	9.8	8.4	7.2	6.4	5.0	3.6	3.2
	accum. var. /%	36.4	46.2	54.6	61.8	68.2	73.2	76.8	80.0
autumn	variance /%	45.5	13.8	7.9	5.1	3.8	2.9	2.6	1.9
	accum. var. /%	45.5	59.3	67.2	72.3	76.1	79.0	81.6	83.5
winter	variance /%	52.9	13.3	8.0	4.1	2.6	2.1	1.6	1.4
	accum. var. /%	52.9	66.2	74.2	78.3	80.9	83.0	84.6	86.0

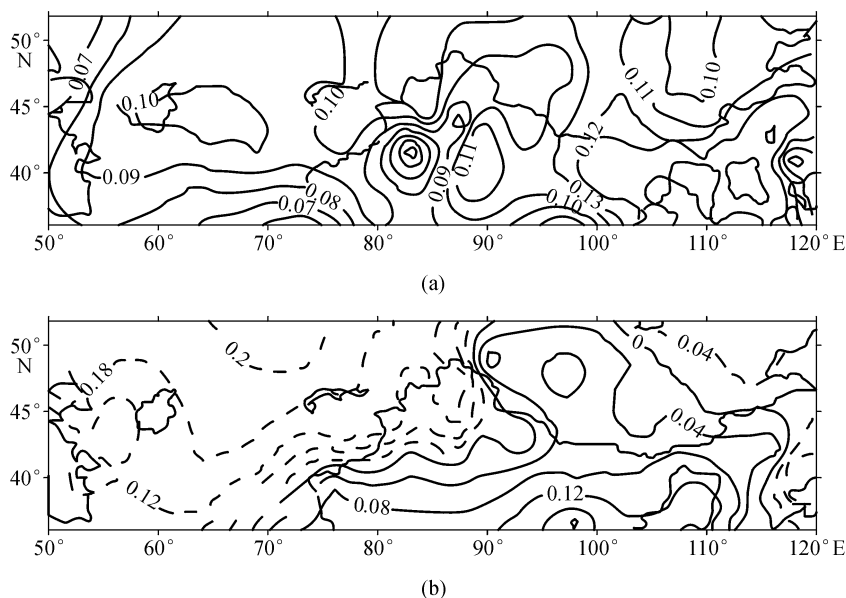


Fig. 2 Spatial distribution of the first (a) and second (b) eigenvectors for the extended mean annual temperature anomalies. The solid and dashed lines denote positive and negative values, respectively.

3.2 REOF-based reconstruction of extended temperature field

In order to study the prominence of the regional differences in temperature variations, the first ten loading vectors of the EOF expansion (explaining 88% of the total variance) were also subjected to a REOF expansion. After rotation, the accumulated variance for the first three rotated loading vectors was 60%, which is useful in describing the regional features of the temperature field. By taking 0.7 as a threshold value for the rotated loading vectors in the REOF, we obtained four sub-regions with anomalous temperature variation in the study area (Fig. 1). They are the East Asia Monsoon Region (I), Central Asia Arid Region (II), Mongolian Arid Region (III), and Tarim Basin Arid Region (IV). The stations near the maximum rotated loading vectors can be regarded as representative stations. Sub-region I covers the region from the southern border of the Badain Jaran Desert to Qinghai Lake in the west, and from the China-Mongolia boarder to the east, including northern China and the eastern part of NW China. The representative station, as indicated by the rotated loading vector, is Yulin (109.7°E, 38.2°N), with a central value of +0.9. Sub-region II is located in the typically central Asia arid region, including Kazakhstan, Uzbekistan, and the northern part of Tajikistan and Turkmenistan. The representative station is Karaganda (73.1°E, 49.8°N), with a central value of -0.84. The sub-region III includes northern Xinjiang and the Hexi Corridor in China, Mongolia and the southern part of Russia. The representative station is Altai (96.2°E, 46.4°N), with a central value of +0.76. Sub-region IV is mainly composed of two inland arid regions, the Tarim Basin in southern Xinjiang and the Qaidam Basin, and the southeastern part of central Asia (Fig. 1). The representative station is Kash (76°E, 39.5°N), with a central value of -0.55. The temperature variations in the four sub-regions are different due to the different influences of multi-scale climate systems. For example, the border of sub-region I is in general agreement with the border of the modern summer monsoon region in China, which is mainly influenced by the East Asian monsoon climate. Sub-regions II–IV are the regions mainly influenced by the westerlies, and different land cover changes in the region.

3.3 Regional difference of temperature changes in the study area

As discussed in section 3.2, the temperature changes in the four sub-regions can be represented by four central representative station series. Figure 3 shows the time series of annual (left panel) and winter (right panel) mean temperature anomalies of the representative stations (a–d) and the whole study area (e) in the interval 1901–2003. It can be seen clearly that a significant warming trend existed in all four sub-regions, as indicated by the first EOF

eigenvector. This warming trend is highlighted by the linear relationship shown in Fig. 3, where the most obvious warming is in region III (Mongolian Plateau Arid Region) (Fig. 3(c)), where the temperature increase rate is 0.23°C per decade. The second distinct warming trend can be seen in region I (East Asian Monsoon Region) (Fig. 3(a)), in which the temperature increase rate is 0.19°C per decade. In central Asia (region II) (Fig. 3(b)) and the Tarim Basin (region IV) (Fig. 3(d)), the rates of temperature increases are 0.16 and 0.15°C per decade, respectively. The temperature variations in the four regions are far greater than the mean value of variation in the whole of China (0.044°C per decade) (Wang et al., 1998; Qian et al., 2001), and are also greater than the updated estimated value (0.058°C per decade) in China (Wang et al., 2004). The average of the increasing amplitudes of the annual mean temperature variations in the study region is 0.18°C per decade and is similar to that over the Tibetan Plateau (0.16°C per decade) (Liu et al., 1998; Liu and Chen, 2000). It is also larger than that of the Northern Hemisphere (0.074°C per decade) and global averages (0.07°C per decade) (Jones and Moberg, 2003). Wang et al. (1998, 2004) found that the regions where temperature increased most significantly in China during the past 100 years were in northeastern, northwestern and northern China as well as the Tibetan Plateau. These regions are fully or partially covered within the study area.

Warming in winter is more significant in the East Asian monsoonal region (Fig. 3(a)) and the Mongolian Plateau (Fig. 3(c)) than in central Asia (Fig. 3(b)) and the Tarim Basin (Fig. 3(d)). It is generally believed that temperature variation in winter contributes more to annual mean temperature changes. The winter mean temperature changes in the study area are in agreement with records from eastern China (Qian et al., 2001) and the Northern Hemisphere (Jones and Briffa, 1992). Additionally, there were differences in the timing and amplitude of temperature changes among the four sub-regions. Negative values are seen in temperature variations in the four sub-regions at the beginning of the 1900s, followed by a warming initiated in the east monsoonal region, central Asia and the Tarim Basin during the 1920s; but this trend was not seen in the Mongolian Plateau (Fig. 3(c)). The warming during the 1940s was much more distinct in the east monsoonal region (Fig. 3(a)), while in the Tarim Basin the temperature increase rate reached 0.025°C per year from the 1930s to 1940s. A larger amplitude of cooling appeared in the late 1940s and early 1950s and it was consistent with previous studies (Wang et al., 1998; Liu et al., 1998; Qian et al., 2001). In central Asia, the warming in 1940s was not obvious, with annual mean temperature only slightly increased after the 1930s. In the Mongolian Plateau, however, the temperature variations showed a continuous steady warming from the early 1900s to the middle 1950s. Then a prominent cooling occurred in the late 1960s (Fig. 3(c)). Consistent temperature changes occurred in all

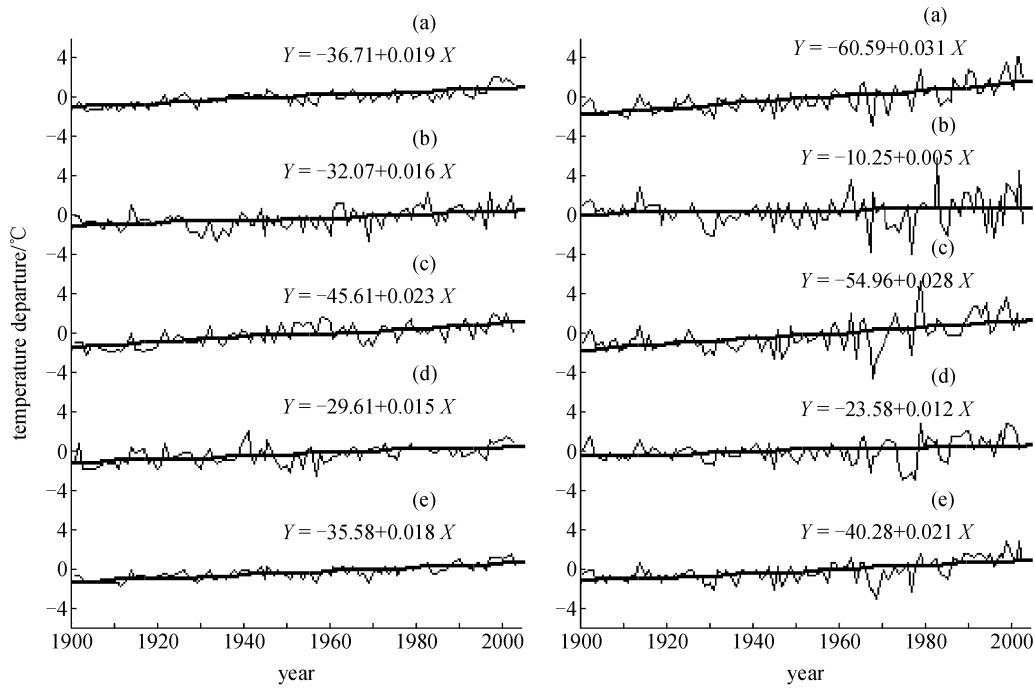


Fig. 3 Annual (left panel) and winter (right panel) mean temperature anomalies of the representative stations ((a) to (d)) and the research area as a whole (e) in the interval 1901–2003. The coarse lines show the linear trends of temperature variation. (a)East Asia Monsoon Region; (b)Central Asia Arid Region; (c)Mongolian Plateau Arid Region; (d)Tarim Basin Arid Region; (e) Regional area in this study

sub-regions after the 1970s. Therefore, the prominent warming in the 1940s reported by previous studies might only appear in eastern China and over the Tibetan Plateau since it is not significant in the arid mid-latitude central Asia and eastern Asia.

3.4 Comparison of temperature variation with tree-ring index series

Here, we show a comparison of the reconstructed temperature time series of Central Asia with a temperature-predominant tree-ring index from sub-region III. The reconstructed temperature series is from Altai, located in region III (Mongolian Plateau) (Fig. 4(b)), and the tree-ring index series from the same region (Jacoby et al., 1996) (Fig. 4(a)). Both the tree-ring index and the reconstructed temperature time series have been smoothed using an 11-year running average. It can be seen from Figs. 4 (a) and (b) that their trends are in good agreement (the correlation coefficient is 0.85 between the 11-year running average data), highlighting a continuous warming trend during the last century. The consistency of these two time series suggests that the EOFs-based temperature reconstruction series can be a reliable record for the last 100 years. Figure 4(c) shows the temperature series average from the observational annual mean temperature series from Almaty (43.2°N, 76.9°E), Tashkent (41.3°N, 69.3°E), and Chardzhev (39.05°N, 63.36°E), which are

adjacent to each other. Figure 4(d) shows the reconstructed temperature series from the same above-mentioned three stations.

Tree-ring research suggests that surface air temperature in central Mongolia has been increasing linearly since the mid-nineteenth century (Jacoby et al., 1996). It shows extraordinary warming in the area during the 20th century, compared with the last 500 years. This warming trend in the Mongolian Plateau may reflect an altitude effect (Altai lies at an altitude of 2147 m a.s.l) due to a probable sensitivity of this station with the increase in temperature (Liu and Chen, 2000), but this may be double-counted on “natural temperature variation”.

3.5 Comparison of temperature variations in study area with other regions

Comparison of the annual mean temperature variations in the study area including the Northern Hemisphere, Tibetan Plateau, eastern China, Xinjiang, and China as a whole is shown in Fig. 5. It reveals that temperature changes have undergone a semi-continuous warming trend. The averaged temperature increase rates in the study area are 0.18°C per decade in summer and 0.21°C per decade in winter, respectively. These changes in temperature are of a greater magnitude than in the other regions of China and are approximately twice the rate of temperature increase in the Northern Hemisphere (0.074°C per decade) (Jones

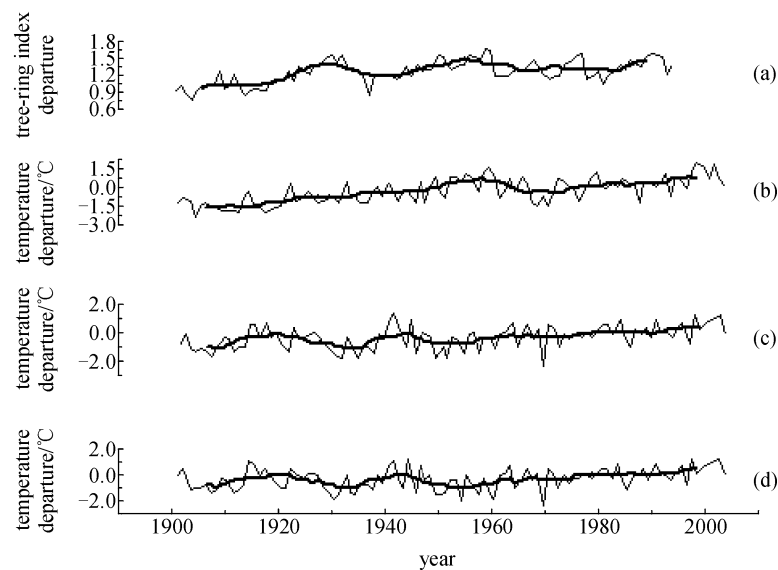


Fig. 4 Comparison of extended temperature time series, tree-rings and observational temperature between 1901 and 2003. The coarse solid line is the 11-year moving averaged series. (a) Tree-ring index departure of Mongolia (after Jacoby et al., 1996); (b) Reconstructed temperature departure of Altai Station (observational data is used in the curve after 1961, the same below); (c) The observational averaged temperature departure of the 3 adjacent stations with 100 years of continuous observation in Central Asia; and (d) Extended temperature departure of the 3 stations in Central Asia.

et al., 1999, Jones and Moberg, 2003). This warming trend is clearly obvious in eastern China (monsoon region), the Tibetan Plateau (high altitude), Xinjiang (westerly influenced region), China as a whole and the Northern Hemisphere (Fig. 5). The accelerated warming since the 1970s in the study area is also consistent with the conclusion that warming is larger but not necessarily more significant in continental regions than over the oceans (Jones and Moberg, 2003).

In this section, when temperature departure is bigger or less than 0°C , the period is defined as a warming or cooling period respectively. Though there are decadal fluctuations of temperature records in the Northern Hemisphere and the Tibetan Plateau, the magnitude of the fluctuations is significantly large in the study area. It is in the order of $0.5\text{--}1^{\circ}\text{C}$ during warm phases and $0.2\text{--}0.5^{\circ}\text{C}$ during cold phases, yielding a net warming of 0.5°C (Fig. 5). The beginning of the 20th century was a period of lower temperature in the mid-latitude Asian arid and semi-arid regions, with the first warming occurring in the 1910s, earlier than that in the Northern Hemisphere and similar to that over eastern China. This warming period lasted until the mid-1920s when the region turned cool, which continued until the early 1930s. The second period of warming occurred after the 1930s and lasted until the early 1940s when temperatures remained relatively constant, but displayed large inter-annual variation. Cooling then began in the mid-1940s, which lasted until the late 1950s (Fig. 5).

In eastern China, the first warming did not start until the 1920s, which peaked in the 1940s, making it a prominent

warming period in this region. The period between the 1950s and the 1970s was then relatively colder, with temperatures further decreasing into the early 1980s (Wang et al., 1998; Qian et al., 2001). The magnitude of temperature change during this period was even larger than that in the Tibetan Plateau (Fig. 5). Liu et al. (1998) found that the warming in the 1940s in the high altitude of the Tibetan Plateau was also prominent, lasting from the 1920s to the 1960s, but the magnitude of warming was not as large as that in eastern China. However, none of the ice core records from the Tibetan Plateau (Yao et al., 1991, 1997; Wang et al., 2003) shows extreme warming during the 1940s. Rather, they reveal a similar continuous warming, which is evidenced by tree-ring indices from Mongolia (Jacoby et al., 1996). The temperature time series developed by Wang et al. (1998) in Xinjiang (Fig. 5) also showed that there was no obvious warming during the 1940s. The results suggested that the warming in the 1940s was restricted to eastern China, since our records from arid mid-latitude Asia did not provide a similar event, and the duration and mechanism of this warming needs further investigation.

The warming trend during the last 100 years in the study area is mainly due to the increased winter temperature, although some studies suggest that the warming is an effect of the urban heat island (Singer, 2003; Singer et al., 2001). However, in the study area industry is undeveloped and the density of human population is relatively small. Therefore, we can discount any influence from heating caused by large urban areas. The contribution of winter temperature

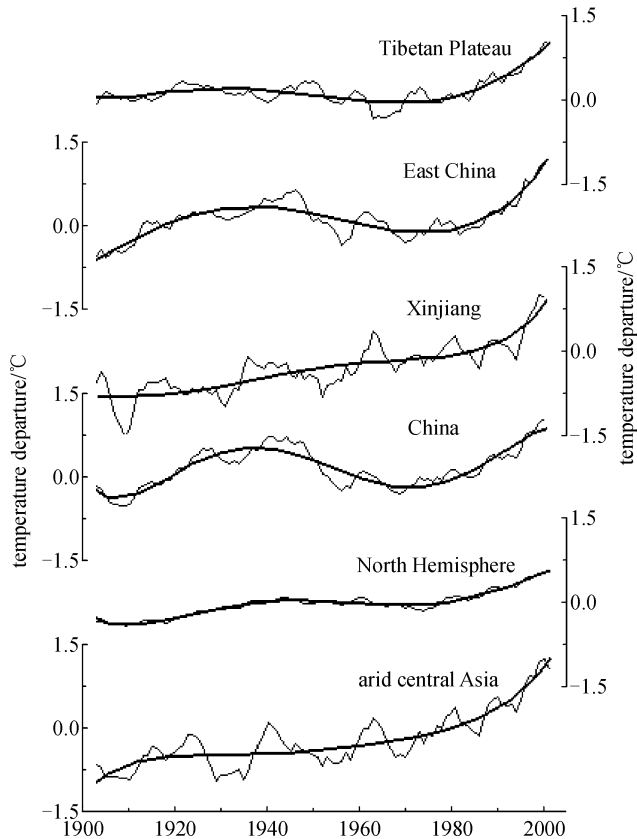


Fig. 5 Comparison of the temperature changes in the mid-east Asian arid area and the Tibetan Plateau (Liu et al., 1998), East China, Xinjiang, China (Wang et al., 2004) and NH (Jones et al., 2003) during the last 100 years. The temperature anomalies (in vertical coordinates in the figure) are all relative to the mean value of 1961–1990 according to Jones et al. (1994). The curves are smoothed with a 5-year moving average. The fine solid line is the 5-year moving average sequence. The coarse solid line is the fitted curve by a quintic polynomial equation. The NH temperature data is from the Climatic Research Unit, East Anglia University, UK. Temperature unit: °C.

to annual mean temperature is also not the same in different periods, although the winter warming amplitude rate has been 0.21°C per decade (Fig. 3) in the study area during the last 100 years. However, there are two anomalous periods. One is in the 1910s, when surface air temperature increased, while the trend in annual mean temperature decreased, resulting in a relatively cold decade. The other period is in the 1950s, lasting as a relatively cold decade. The winter temperature increased over central Asia and Xinjiang in China, and the increased summer mean temperature suggests that this season is important in the annual mean temperature. Figure 3 indicates that the winter warming contributes to the increasing rate of mean annual temperature. Overall, the trend of winter temperature change is important in determining the annual mean temperature in the study area, with the exception of some individual periods.

4 Conclusions

A temperature series is extended from 1960 back to 1901 based on an EOF expansion method (Tu, 1986). REOF analysis is also used to divide the study area into four sub-regions. All sub-regions show a distinct warming trend, with linear fitted warming rates by 0.19°C per decade, 0.16°C per decade, 0.23°C per decade and 0.15°C per decade, respectively. The most prominent warming occurs in the Mongolian Plateau Arid Region. The warming rate in the study area, as a whole, is 0.18°C per decade, which is larger than the rate identified over averaged China (0.058°C per decade, Wang et al., 2004) and the average global warming rate (0.07°C per decade, Jones and Moberg, 2003), and is similar to that of the Tibetan Plateau (0.16°C per decade, Liu et al., 1998). The most noticeable trend in temperature change from the study area is in the winter temperature variation, which has increased at a rate of 0.21°C per decade and is greater than the mean annual increasing rate (0.18°C per decade). Thus, the annual warming is a function of changes in winter temperature, although there appears to be an exception notably during the 1910s and 1950s.

The warming process in the study area during the last 100 years has two stages: a relatively slow increase in temperature between the 1900s and the 1970s (0.13°C per decade) and a rapid increase in temperature after the 1970s (0.4°C per decade). Five distinct warming cycles that last approximately ten to twenty years can be identified in the records, with oscillations occurring in the 1920s, 1940s, 1960s, 1980s, and 1990s. The mechanism of temperature change in central Asia and the differences among the regions is unclear. Instrumental data as well as climate modeling experiments are needed for further investigation.

Acknowledgements This research work was supported by the National Natural Science Foundation of China (NSFC) Innovation Team Project (Grant No. 40421101), the NSFC Outstanding Young Scholars Project (No. 40125001), and the National Key Project of the Ministry of Science and Technology (2002CB714004). It was also funded by the Ten Talents Projects, Gansu Provincial Meteorological Bureau.

References

- Ding Y H, Dai X S (1994). Temperature change in China during the past 100 years. *Meteorology*, 20(12): 19–26 (in Chinese)
- Ding Y H, Wang S R (2001). A Survey of climate change and the ecological environment in Northwest China. Beijing: Meteorological Press, 204 (in Chinese)
- Folland C K, Rayner N A, Brown S J, Smith T M, Shen S S P, Parker D E, Macadam I, Jones P D, Jones R N, Nicholls N, Sexton D M H (2001). Global temperature change and its uncertainties since 1861. *Geophysical Research Letters*, 28: 2621–2624
- Hansen J E, Ruedy R, Glascoe J (1999). GISS analysis of surface

- temperature change. *Journal of Geophysical Research*, 104: 30997–31022
- Hansen J, Ruedy R, Sato M, Imhoff M, Lawrence W, Easterling D, Peterson T, Karl T (2001). A closer look at United States and global surface temperature change. *Journal of Geophysical Research*, 106: 23947–23963
- Huang J Y (1998). EOF analysis and its application in weather analysis. *Meteorology*, 14(9): 47–51 (in Chinese)
- Jacoby G C, Rosanne D D, Davaajamts T (1996). Mongolian tree rings and 20th-century warming. *Science*, 273: 771–773
- Jones P D (1994). Hemispheric surface air-temperature variations—a reanalysis and an update to 1993. *Journal of Climate*, 7 (11): 1794–1802
- Jones P D, Briffa K R (1992). Global surface air temperature variations over the twentieth century, 1, Spatial, temporal and seasonal details. *Holocene*, (2): 165–179
- Jones P D, Moberg A (2003). Hemispheric and large-scale surface air temperature variations: An extensive revision and an update to 2001. *Journal of Climate*, 16: 206–223
- Jones P D, New M, Parker D E, Martin S, Rigor I G (1999). Surface air temperature and its changes over the past 150 years. *Reviews of Geophysics*, 37 (2): 173–199
- Kawamura R (1994). A rotated EOF analysis of global sea-surface temperature variability with interannual and interdecadal scales. *Journal of Physical Oceanography*, 24: 707–715
- Lin X C, Yu S Q, Tang G L (1995). Temperature sequence of China for the past 100 years. *Atmospheric Sciences* 19(5): 525–534 (in Chinese)
- Liu X D, Chen B D (2000). Climatic Warming in the Tibetan Plateau during Recent Decades. *International Journal of Climatology*, 20: 1729–1742
- Liu X D, Zhang M F, Hui X Y, Kang X C (1998). The features of contemporary climate change on the Tibetan Plateau and its response to greenhouse effects. *Geographical Sciences*, 18(2): 113–121 (in Chinese)
- Peterson T C, Karl T R, Jamason P F, Knight R, Easterling D R (1998). First difference method: Maximizing station density for the calculation of long-term global temperature change. *Journal of Geophysical Research-Atmosphere*, 103 (D20): 25967–25974
- Qian Z A, Wu T W, Song M H, Ma X B, Cai Y, Liang X Y (2001). Arid disaster and advances in arid climate researches over northwest china. *Advances in Earth Sciences*, 16(1): 28–38 (in Chinese)
- Servain J, Legler D M (1986). Empirical orthogonal function analyses of tropical Atlantic sea-surface temperature and wind stress: 1964–1979. *Journal of Geophysical Research*, 91(C12): 14181–14191
- Singer S F (2003). Editor bias on climatic change. *Science*, 301:595–596
- Singer S F, Kennedy D, Johnston J D (2001). Global warming: An insignificant trend? *Science*, 292 (5519): 1063–1064
- Solomon S, Qin D, Manning M, Chen Z, Marquis M, Averyt K B, Tignor M, Miller H L (2007). Technical Summary. In: Solomon S, Qin D, Manning M, Chen Z, Marquis M, Averyt K B, Tignor M, Miller H L editors, *Climate Change 2007: The Physical Science Basis. Contribution of Working Group I to the Fourth Assessment Report of the Intergovernmental Panel on Climate Change*. Cambridge University Press: Cambridge, United Kingdom and New York, NY, USA
- Tu Q P (1986). A method for extending the temperature sequence field. *The journal of Nanjing Meteorological College (in Chinese)*, 9(1): 19–30
- Tu Q P, Deng Z W, Zhou X L (2000). Regional Characteristics of the temperature anomaly in China. *ACTA Meteorologica*, 58(3): 288–296 (in Chinese)
- Wang N L, Yao T D, Pu J C, Ren J W, Zhang Y L (2003). Temperature change during the last 100 years documented by Malan Ice Core on the Tibetan Plateau. *Chinese Science Bulletin*, 48(11): 1219–1233 (in Chinese)
- Wang S W (1990). The trend of temperature change in China and the globe for the past 100 years. *Meteorological Monthly*, 16(2): 11–15 (in Chinese)
- Wang S W, Ye J L, Gong D Y, Zhu J H, Yao T D (1998). Construction of mean annual temperature series for the last one hundred years in China. *Journal of Applied Meteorology (in Chinese with English abstract)*, 9(4):393–401
- Wang S W, Zhu J H, Cai J N (2004). Interdecadal variability of temperature and precipitation in China since 1880. *Advances in Atmospheric Sciences*, 21(3): 307–313
- Yao T D, Shi Y F, Thompson L G (1997). High resolution record of paleoclimate since the little ice age from the Tibetan ice cores. *Quaternary International*, 37: 19–23
- Yao T D, Xie Z C, Wu X L, Thompson L G (1991). Climatic-change since little ice-age recorded by Dunde ice cap. *Science in China (Series B)*, 34(6): 760–767
- Zhu Q G, Shi N, Wu Z H, Shen T L (1997). The long-term change of atmospheric active centers in northern winter and its correlation with China climate in recent 100 year. *ACTA Meteorologica Sinica*, 55(6): 750–758 (in Chinese)